Physics 575
Accelerator Physics and Technologies for Linear Colliders
Winter 2002
Chapter 5 – Damping Rings

L. Emery
Argonne National Laboratory

February 7th, 2002

Contents

5.1 Introduction

Damping rings are used in linear colliders to quickly reduce the emittance of the electron and positron beams at an early stage of the acceleration. A damping ring is a storage ring optimized for a fast damping time and a low emittance.

A train of bunches is injected into the damping ring from a transport line. After several thousands of turns, the bunches will have been reduced in the transverse dimension, and then are extracted into a transport line leading to a linac for further acceleration.

Expressed in an equation,

$$\varepsilon_x(t) = \varepsilon_{x,\mathrm{inj}} e^{-2t/\tau_x} + \varepsilon_{x,\mathrm{eq}}(1 - e^{-2t/\tau_x}), \tag{5.1}$$

where $\varepsilon_{x,\mathrm{inj}}$ is the injected emittance, $\varepsilon_{\mathrm{eq}}$ is the equilibrium emittance, and similarly for y. τ_x is the damping time for the particle motion. Note that the beams may be stored for only a few damping times such that the extracted emittance is somewhat larger than the equilibrium emittance.

As shown in Figure 5.1, a storage ring is essentially a curved beamline of dipole magnets (for bending) and quadrupole magnets (for focusing) that closes on itself. Usually the magnets are laid out as an oval: two semi-circles and two straight sections. However a "dog bone" layout is proposed for the TESLA linear collider [1] in order to fit the straight sections side-by-side in the main linac tunnel to save costs.

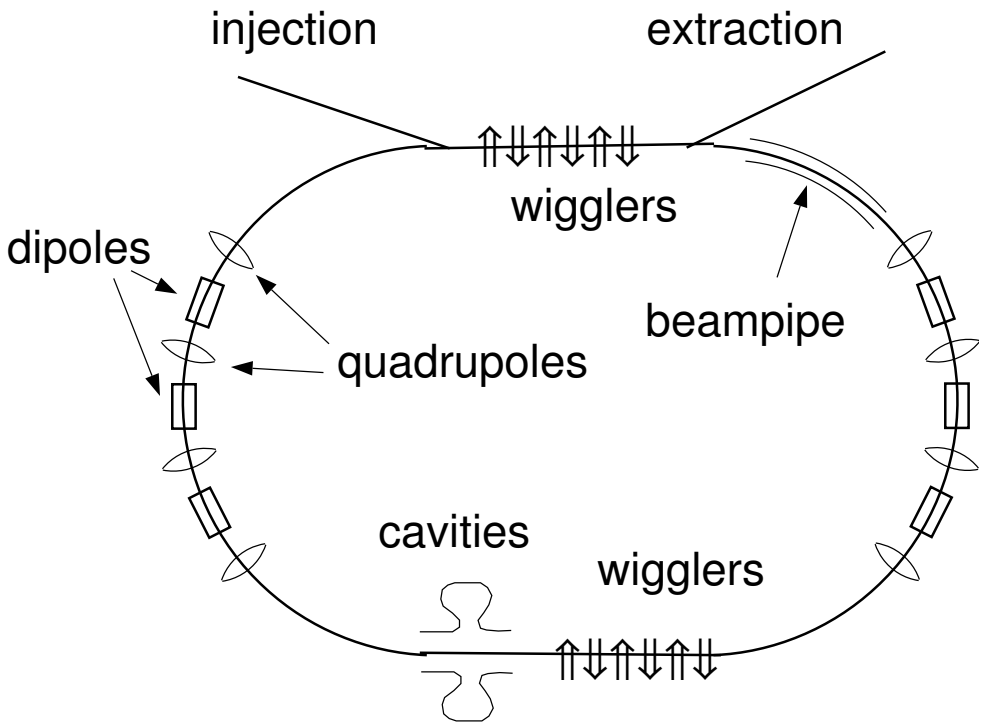

Figure 5.1: Layout of essential damping ring.

Additionally, a storage ring requires rf cavities for replacing particle energy lost through synchrotron radiation and for maintaining the bunching structure.

Damping occurs in all electron storage rings through the combination of emission of synchrotron radiation and energy recovery by an rf cavity. In time, an equilibrium in beam size is established when the trajectory "noise" created by emitting photons randomly, a diffusion process, matches the damping rate.

The arrangement and strength of the dipoles and the quadrupoles (called the lattice) to be determined by the accelerator designers partly determine the damping rate and the equilibrium beam parameters of transverse emittance and energy spread. In general the stronger the dipoles, the faster the damping rate, and the stronger the quadrupoles, the smaller the emittance.

Special magnets called wigglers are inserted in straight sections of the damping rings to significantly increase the damping rate and lower the emittance as an alternative to using difficult-to-achieve optics.

Sextupoles magnets (i.e., with six poles) are required for correcting chromatic aberrations (focal length change for particles of different momentum). These sextupoles have a drawback in that they add nonlinearities to the particle motion, which cause particle motion instability when a particle is launched at a large enough offset from the design orbit and effectively reduce the usable aperture of the beampipe. Strongly focusing lattices such as those in damping rings require stronger sextupoles, and therefore may have aperture problems.

Almost all design parameters of the storage ring are interrelated, sometimes at cross purposes. These will be reviewed in this lecture using some designs proposed for the NLC [2] and TESLA [1] damping rings.

5.2 Storage Rings Optics

5.2.1 Bending

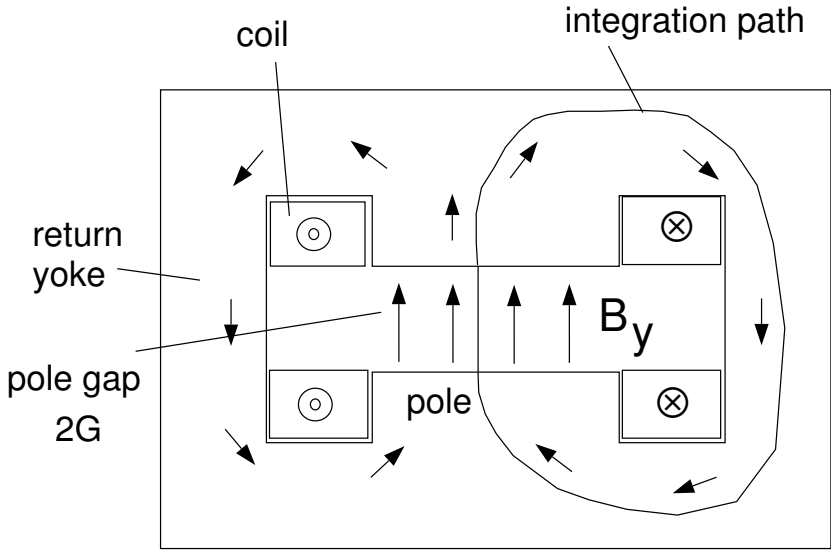

Figure 5.2: Dipole cross section showing integration path.

The particles are deflected into arcs of a circle by an iron dipole magnet with a uniform field inside a gap of height $2G$. The magnetic field is generated by the current in the coils wrapped around an iron pole. A yoke provides a path for the magnetic field lines.

The uniform field is determined by a path integral shown in Figure 5.2,

$$\oint \vec{H} d\vec{l} = 2GB_y + \int_{\text{iron}} \frac{\vec{B}}{\mu} d\vec{l} = \frac{4\pi}{c} 2I, \tag{5.2}$$

where μ is the permeability of the iron, and I is the current through one coil. Since we operate with reasonable fields such that μ is very large, the path integral can be dropped, and

$$B_y = \frac{4\pi}{c} \frac{I}{G} \tag{5.3}$$

or

$$B_y[\text{T}] = \frac{0.4\pi}{10^4} \frac{I[\text{A-turn}]}{G[\text{cm}]}. \tag{5.4}$$

For a field of 2 T and a gap of 2 cm, the coil current is 31 kA-turn. Say for a coil of 50 turns, the circuit current needs to be 620 A. A smaller gap would need less current, but a large vertical aperture of usually 2 cm is required for injecting the beam.

The bending radius of the arc of the trajectory is

$$\frac{1}{\rho} = \frac{eB_y}{pc} \tag{5.5}$$

or

$$\frac{1}{\rho[\text{m}]} = \frac{0.3 B_y[\text{T}]}{E[\text{GeV}]}. \tag{5.6}$$

For a 1.2-GeV beam, the bending radius from 2 T is 2.0 m.

Saturation effects in the iron start to occur at 1.6 T, and the magnet is saturated at about 2 T, meaning that increasing the current from that point on will not increase the field efficiently. Designs should avoid requiring fields larger than 2 T. Higher fields can be produced by superconducting magnets, but they are much more expensive and are complicated to operate.

5.2.2 Focusing

Quadrupole magnets are installed in spaces betweeen dipole magnets and focus particle trajectories using a gradient in the magnetic field. An idealized cross section of the quadrupole magnet poles is given in Figure 5.3. Because $dB_y/dx = dB_x/dy$, a magnet that focuses in the horizontal plane will defocus in the vertical plane. By alternating the polarity of the magnets in a

beamline or arc, one can achieve overall focusing with the requirement that the quadrupole magnets have to be spaced at intervals significantly shorter than the focal length.

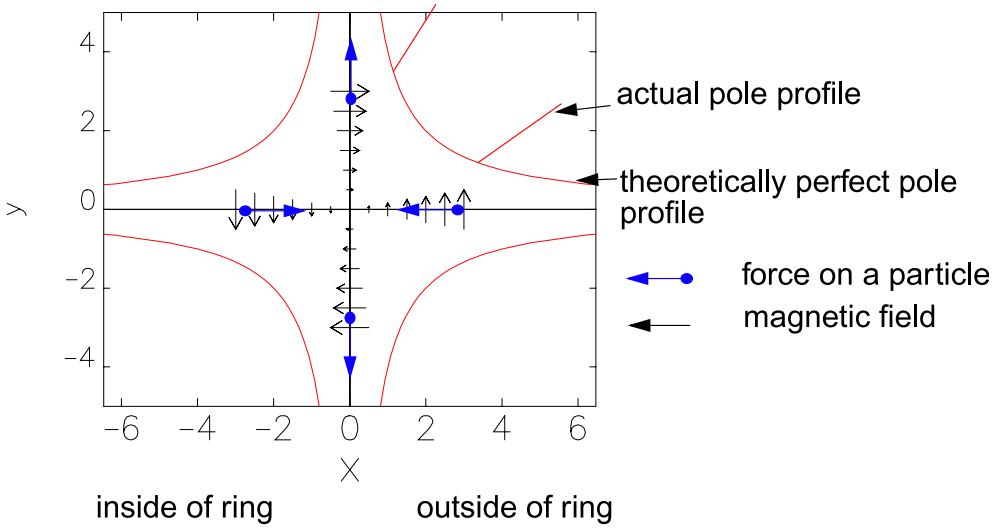

Figure 5.3: Quadrupole cross section showing forces on particles on x- and y-axes.

As mentioned earlier, iron saturates at about 2 T. In a quadrupole the saturation would first occur somewhere along the long poles. To avoid saturation, the field at the pole tip should not be larger than 1 T.

Another (obvious) design limitation is that the pole tip radius R must be larger than the required aperture for the beam.

Both these limitations determine the maximum gradient of a quadrupole. The normalized strength k of a quadrupole, which is used in optics calculations, is determined by the energy of the beam.

As an example, say that R = 3 cm, $B_{\rm tip}$ = 1 T, E = 2 GeV, and l_Q = 0.2 m. We use $g = B_{\rm tip}/R$, $k[{\rm m}^{-2}] = 0.3g[{\rm T/m}]/E[{\rm GeV}]$, and $f = 1/(kl_Q)$ as the focal length to give g = 33 T/m, k = 5 m^{-2}, f = 1 m.

5.2.3 Betatron Oscillation

Betatron oscillations are the pseudo-sinusoidal motion of a particle relative to the design trajectory; they are "shaped" by the focusing channel of the

beamline or ring and are due to the initial coordinates of the particles. See Figure 5.4 for examples trajectories through a FODO channel. The amplitude of betatron oscillations decrease during the damping process, giving a beam distribution that gets smaller and smaller. When a particle occasionally emits a high-energy photon, the particle starts a new oscillation with a higher amplitude. Since the radiation process is continual, the amplitude step-changes occur forever, but the accumulated amplitude is limited because of the damping process.

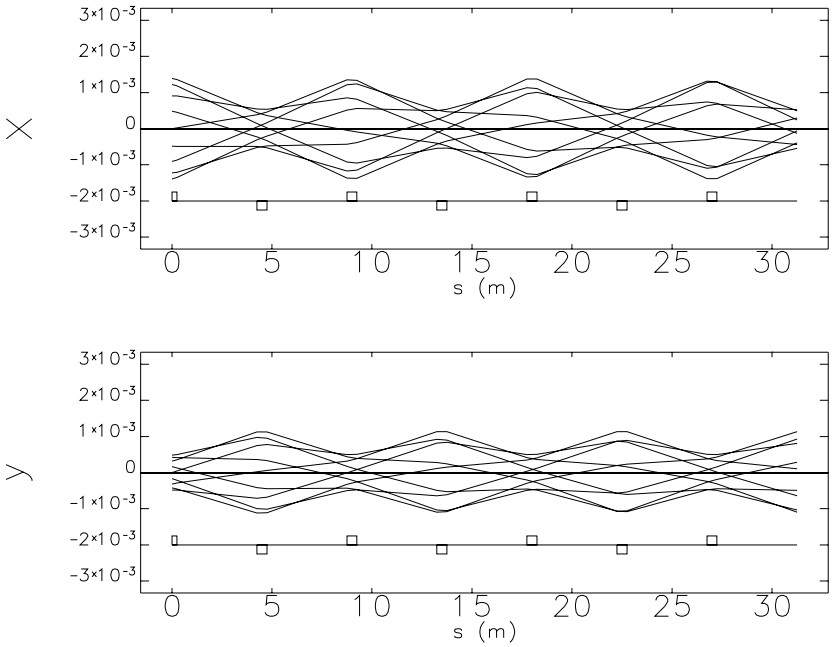

Figure 5.4: FODO channel with several x and y trajectories of different initial conditions.

However it is useful to describe the motion in the absence of the radiation effects.[1] Omitting other complicating terms like a curvature term in x plane, magnet errors, and sextupole magnets, the equation of motion for x and y coordinates relative to the design axis are

$$x'' + k(s)x = 0 \text{ and} \tag{5.7}$$

[1]In the case of a proton, there is little or no radiation emission, so a betatron oscillation is the correct description of the motion of a single particle.

$$y'' - k(s)y = 0, \tag{5.8}$$

where $k(s)$ is the focusing strength of the quadrupole along the beamline or arc, which is a piecewise function. The general solution looks like that of a harmonic oscillator,

$$x(s) = A_x\sqrt{\beta_x}\cos(\phi_x(s) + \phi_{x0}), \tag{5.9}$$

$$y(s) = A_y\sqrt{\beta_y}\cos(\phi_y(s) + \phi_{y0}), \tag{5.10}$$

where the β's are an envelope function (called the beta function) of length dimension, are always positive, and may be totally different in character for each plane. The ϕ functions are called the phase advance defined by the β's,

$$\phi = \int_0^s ds/\beta(s), \tag{5.11}$$

which increases monotonically with s and is not necessarily linear in s. When ϕ increases by 2π along s, then we say the particle has executed one betatron oscillation. The value of ϕ at $s = C$ is called the betatron number, which is the number of oscillations in one turn. This betatron number is not necessarily a whole number, and actually should not be a whole number in order to avoid amplitude-growing resonances seeded by magnet errors.

In a storage ring, we select a reference location to be s = 0, and solve for the β as a periodic function, $\beta|_{s=0} = \beta|_{s=C}$. Given the complicated nature of $k(s)$, $\beta(s)$ and $\phi(s)$ are solved numerically by a computer program.

In a ring with a constant k, then β is constant (β would be equal to $1/\sqrt{k}$), and $\phi(s) = \sqrt{k}s$, as for a pure harmonic oscillation.

It turns out that the β function is a very useful quantity in beam dynamics. It is not only used for the solution of a particular trajectory but also used to describe the distribution of particles around the ring. It comes up also in studies of tolerances to magnet errors and instabilities of the beam.

The values of $x'(s)$ and $y'(s)$ are obtained by differentiating with respect to s:

$$x'(s) = A_x\left(-\frac{1}{\sqrt{\beta_x}}\sin(\phi_x(s) + \phi_{x0}) + \frac{\beta_x'}{\sqrt{\beta_x}}\cos(\phi_x(s) + \phi_{x0})\right), \tag{5.12}$$

$$y'(s) = A_y\left(-\frac{1}{\sqrt{\beta_y}}\sin(\phi_y(s) + \phi_{y0}) + \frac{\beta_y'}{\sqrt{\beta_y}}\cos(\phi_y(s) + \phi_{y0})\right), \tag{5.13}$$

which is messy but allows us to introduce the concept of the invariant of the motion and the phase ellipse. If we eliminate the phases, we get a constant of the motion for each plane,

$$\gamma_x x^2 + 2\alpha_x x x' + \beta x'^2 = A_x^2, \tag{5.14}$$

where $\alpha_x(s) = \beta'(s)/2$ and $\gamma_x(s) = (1 + \alpha_x(s)^2)/\beta_x(s)$, and similarly for y. The collection of β, α, and γ are called the Courant-Snyder parameters or the machine functions. In the x-x' plane the trajectory will be represented by a particular point on the ellipse, as shown in Figure 5.5. As we travel around the ring going through various focusing elements, the coordinates will move as a point on different ellipses, since the machine functions are a function of s.

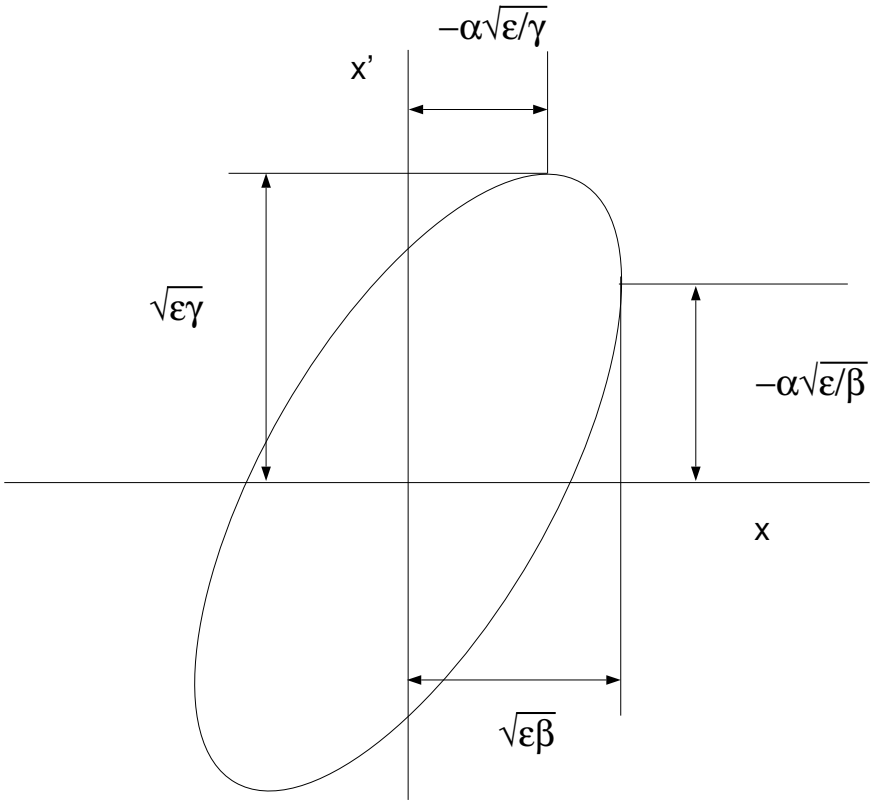

Figure 5.5: Trajectory ellipse dimensions with β, α, and γ and ϵ as the invariant.

At a particular location s around the ring, the betatron oscillation will

occupy different points on the same ellipse on different passes. The ellipse will be eventually be filled out after a large number of passes. Note that we have only considered linear motion so far. The inclusion of sextupoles and nonlinear terms will deform this ellipse.

5.2.4 Phase Space

The transverse coordinates of a particle circulating in a ring are (x, x', y, y') and are measured relative to a reference particle on the design trajectory. x' is defined p_x/p_z and similarly for y'. These are the coordinates of phase space. Strictly speaking, the pairs of coordinates of phase space should be canonical pairs, but since $p_z \approx p_0$ then the two alternatives are equivalent. One may add the longitudinal coordinates, (τ, $\delta = (p - p_0)/p_0$), where τ is the time displacement from a particle synchronous with the rf system.

At "equilibrium" the distribution of particles in phase space at any fixed particular point in the ring is constant, and is Gaussian in character, i.e., $\psi(x) \sim \exp\{-x^2/2\sigma_x^2\}$, and similarly for the other coordinates.

The full distribution function is

$$\psi(x, x', y, y') = A \exp\left\{-\frac{\beta_x x'^2 + 2\alpha_x x x' + \gamma x^2}{\varepsilon_x}\right\} \tag{5.15}$$

$$\times \exp\left\{-\frac{\beta_y y'^2 + 2\alpha_y y y' + \gamma y^2}{\varepsilon_y}\right\}. \tag{5.16}$$

Areas of phase space of constant density of particles are elliptical bands described by the β, α, and γ functions. The density of particles in the neighborhod of a particular trajectory doesn't change as the beam travels along the ring circumference (assuming equilibrium conditions). The area enclosed by one standard deviation of the distribution is π times the emittance ε.

One can also express the beam size as $\sigma_x = \sqrt{\varepsilon_x \beta_x}$, which is a function of s. Given the solution of Equation (5.9), it is not surprising that $\sigma_x \sim \beta_x$. The divergence of the beam is $\sigma'_x = \sqrt{\varepsilon_x \gamma_x}$. Similarly for y.

5.2.5 Dispersion

The dipole magnet strengths are set such that a particle with the design momentum follows a central trajectory through the dipoles and quadrupoles. Particles in a beam actually have a distribution in momentum. Taking p_0

as the design momentum, and p as the momentum of a particle, then $\delta = (p - p_0)/p_0$ is the relative momentum error. In an electron storage ring, the rms momentum spread σ_δ is of the order of 10^{-3}.

Each particle will in general execute a betatron oscillation about a reference orbit particular to the momentum error, i.e., $x_\delta(s) = \eta(s)\delta$, where $\eta(s)$ is a proportionality function called the dispersion (or "eta") function.

The equation for the periodic x_δ and η looks like the equation from which betatron motion was solved, but has the dipole strength as driving terms:

$$x_\delta'' + kx_\delta = \delta/\rho \text{ , or} \tag{5.17}$$

$$\eta'' + k(s)\eta = 1/\rho. \tag{5.18}$$

Since the RHS's of the above equations are nonzero, the dispersion solution does not have arbitrary amplitude and phase as in the betatron oscillation solution. The dispersion is generally positive so that a particle with higher momentum travels on the outside of the design trajectory. We'll see later that for a low-emittance ring, η should in general be made small, which means that the $1/\rho$ driving terms should be small.

5.2.6 Sextupoles and Nonlinearities

Sextupole magnets correct the focusing error of quadrupoles for particles with a momentum error. The sextupoles are located where dispersion is nonzero, so that particles of a given momentum error get either an additional negative or a positive focusing from the sextupolar field.

The sextupoles are more efficient when the dispersion is large. To see this, we rewrite the equation of motion for an off-momentum particle and with a new term for the sextupole

$$x'' + kx = \delta kx - \frac{1}{2}mx^2, \tag{5.19}$$

where $m = (e/cp)d^2B_y/dx^2$ and where we used $k/(1+\delta) = k - \delta k$. Applying $x = x_\beta + x_\delta = x_\beta + \eta\delta$, and collecting only the terms linear in x_β:

$$x_\beta'' + kx_\beta = \delta kx_\beta - m\delta\eta x_\beta \tag{5.20}$$

$$= \delta(k - m\eta)x_\beta. \tag{5.21}$$

Without sextupoles (m=0) the term $\delta k x_\beta$ is a gradient error and causes a tune change that may lead to an instability. The $m\eta$ term can be used to cancel the chromatic aberration. The normalized sextupole strength required here is $m = k/\eta$. Since the sextupoles introduce the nonlinear terms seen in Equation (5.19), it is clear that the sextupoles should be located where the η is large.

We have to correct the chromaticity for both x and y planes. Unfortunately, a sextupole that corrects the focusing error in x worsens the error in y, in analogy to the quadrupoles' effect on focusing. Therefore we need two families of sextupoles with opposite polarities arranged throughout the lattice to compensate both planes. Because the two sets of sextupoles partially offset each other, they need to run at slightly higher strength. The degree that they do depends on the particular lattice cell. This is a critical consideration for choosing a cell type.

We'll see in the next section that for a small emittance, η must be small in the dipoles. However since the bending radius drives the value of η overall, a compromise must be reached between weaker sextupoles and small emittance.

5.3 Radiation Effects

5.3.1 Energy Oscillation

A particle with a momentum error going once around the ring will have travelled over a shorter or a longer path than that of on-momentum particles. The path length difference comes from the extra trajectory through the dipoles where the reference trajectory is curved, and is expressed concisely with

$$\Delta L/L = \alpha_c \delta, \tag{5.22}$$

where $\alpha_c = \int \eta/\rho \, ds$ is called the momentum compaction factor. A particle with positive momentum deviation will arrive late. Since all particles travel at essentially the same velocity c, particles with a momentum spread initially bunched in time will spread out significantly in time (and in longitudinal coordinate) after several turns. If the bunching of particles is destroyed, then the "bunch" can't be accelerated efficiently in a linac upon extraction of the damping ring.

One or more rf cavities (see Figure 5.6 for a typical side view cross section) are used to maintain the bunching (and to maintain the particles' energies

after synchrotron radiation emission). The desired function is adding or subtracting from the energy of a particle according to how much the particle has moved away from the ideal longitudinal position. This restoring action results in an oscillation in the time displacement coordinate and the energy.

An rf cavity produces an oscillating longitudinal electric field that is synchronized with the passage of the bunches. This implies that the driving rf frequency must be a multiple of the particle revolution frequency. We normally speak in terms of the rf voltage ($V = \int E_z \, dz$) since the particles integrate the E-field as they pass through a gap. Figure 5.6 shows an energy gain of U, which is e times the voltage.

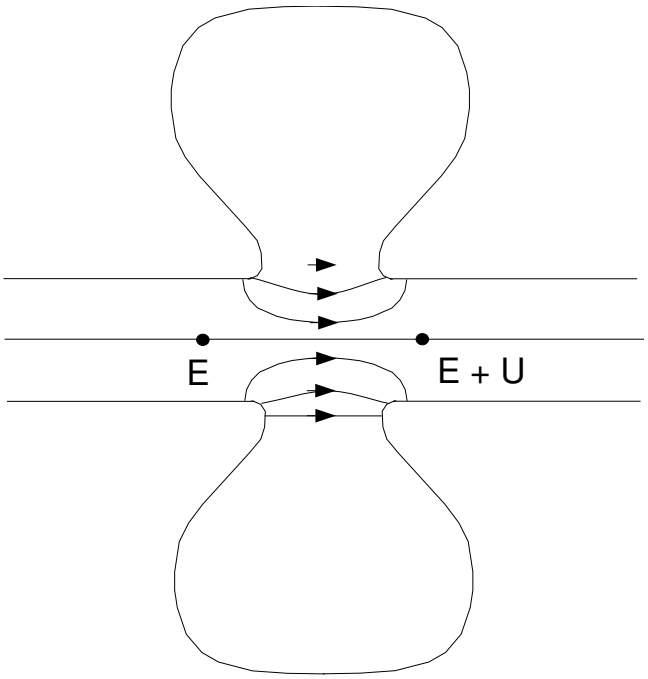

Figure 5.6: Cavity cross section showing the accelerating E-field.

The energy gained for a particle will depend on its position relative to a reference (synchronous) particle passing through the right rf phase for an energy balence with synchrotron radiation.

Say that

$$V(t) = V_0 \cos(2\pi f_{rf} t), \tag{5.23}$$

where $f_{\mathrm{rf}} = h f_0 = h/T_0$ and where h is the rf harmonic number, which is an integer that is usually pretty large since f_{rf} is chosen in the 350 to 750

Mhz range and f_0 is of the order 1 MHz. Note that we took the rf fields as the time reference. Then a synchronous particle that loses energy U_0 from synchrotron radiation must pass through at some time t_s or phase ϕ_s to maintain its energy:

$$U_0 = eV(t_s) = eV_0 \cos(2\pi f_{\text{rf}} t_s) = eV_0 \cos(\phi_s). \tag{5.24}$$

Say that a particle is ahead of the synchronous particle by an amount $c\tau$, where τ is defined the time displacement coordinate. Then the voltage seen by this particle is $V(t_s - \tau)$, i.e., the particle arrived at the cavity ahead of the "correct" time. The total energy gain in one turn for this particle is then

$$\Delta E(\tau) = eV(t_s - \tau) - U_0 = eV_0(\cos(2\pi f_{\text{rf}}(t_s - \tau)) - \cos(2\pi f_{\text{rf}} t_s)). \tag{5.25}$$

For small τ,

$$\Delta E(\tau) = 2\pi f_{\text{rf}} eV_0 \sin(\phi_s)\tau, \tag{5.26}$$

where $-2\pi f_{\text{rf}} V_0 \sin(\phi_s)$ is the slope of the rf voltage at ϕ_s. A particle with $\tau > 0$ will have absorbed too much energy on this pass. The path length will be greater and the particle will arrive later on the next pass, which brings the particles closer to the reference particle. On the second pass the energy gain will not be as much, but the trend in arriving later (and closer to the reference particle) will continue until the "correct" energy is gained. This describes the start of an oscillation, which is depicted in Figure 5.7.

Equation (5.26) shows a linear dependence of energy gain on the time coordinate. Assuming slow changes in coordinates at every turn, this equation and the one for ΔL can both be turned into coupled first-order differential equations which then gives a second-order equation for δ and τ.

The equation for ΔE can be changed into one for $\dot{\delta}$ using $\Delta X \to T_0 \dot{X}$:

$$\dot{\delta} = \frac{2\pi f_{\text{rf}} eV_0 \sin(\phi_s)}{T_0 E}\tau. \tag{5.27}$$

Taking Equation (5.22) and the change in τ, $\Delta\tau = -\Delta L/c$ (remember a longer path means that the particle is falling behind), we get

$$\dot{\tau} = -\frac{L\alpha_c}{cT_0}\delta = -\alpha_c \delta. \tag{5.28}$$

Combining,

$$\ddot{\delta} = -\frac{2\pi\alpha_c f_{\text{rf}} eV_0 \sin(\phi_s)}{T_0 E}\delta, \tag{5.29}$$

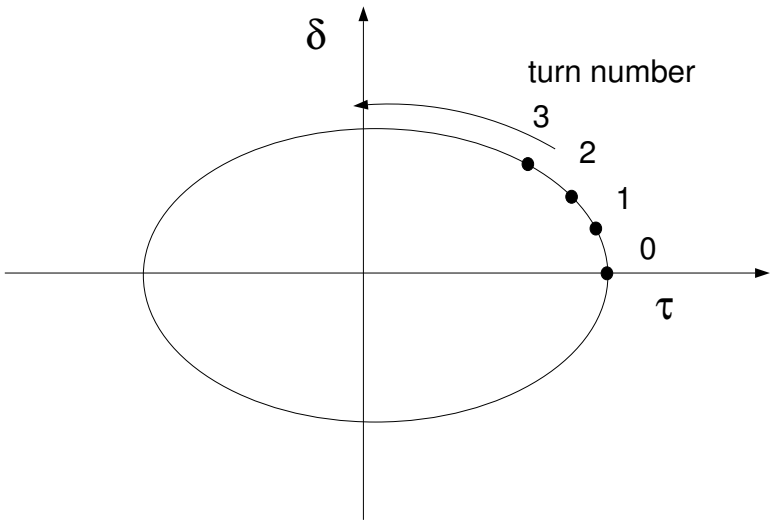

Figure 5.7: Motion in the longitudinal plane following an ellipse.

and similarly for τ.

We define the synchrotron frequency Ω with

$$\Omega_s^2 = \frac{2\pi\alpha_c f_{\rm rf} eV_0 \sin(\phi_s)}{T_0 E}. \tag{5.30}$$

$\Omega_s/2\pi$ is of the order 2 kHz for large rings (the Advanced Photon Source).

The amplitude of the oscillation described above is constant under our assumption. A damping term has been left out by omitting the dependence of energy loss (U_0) on the energy of the particle. This will be covered later.

5.3.2 Synchrotron Energy Loss

The instantaneous power loss by a particle in a magnetic field goes as E^2B^2 and may be expressed in terms of bending radius ρ,

$$P_\gamma[\text{GeV/sec}] = \frac{cC_\gamma}{2\pi}\frac{E^4[\text{GeV}]}{\rho^2}, \tag{5.31}$$

where

$$C_\gamma = \frac{4\pi}{3}\frac{r_e}{(mc^2)^3} = 8.85 \times 10^{-5}\text{m/GeV}^3. \tag{5.32}$$

The energy loss per turn is

$$U = \frac{\langle P_\gamma \rangle}{T_0} = \frac{C_\gamma E^4}{2\pi} \int \frac{ds}{\rho^2}. \tag{5.33}$$

In practical units for a ring with only one type of dipole,

$$U[\text{MeV}] = 0.088 \frac{E^4[\text{GeV}^4]}{\rho[\text{m}]}. \tag{5.34}$$

The quantity U_0 used earlier is U evaluated for $E = E_0$.

Another useful radiation quantity is the photon critical energy, the point in the energy spectrum at which the power emitted below is equal to the power emitted above:

$$u_c = \frac{3}{2} \frac{\hbar c}{\rho} \gamma^3. \tag{5.35}$$

This gives an upper bound to the photon energy in the spectrum. In practical units, $u_c[\text{keV}] = 0.665 E^2[\text{GeV}^2] B[\text{T}]$.

5.3.3 Damping of Energy Oscillations

In the previous description of energy oscillation, we assumed that the energy loss per turn was a constant, U_0, i.e., not dependent on energy. When we add this dependence, a damping term will appear.

Return to Equation (5.25) and replace U_0 with

$$U(E) = U_0 + \left.\frac{dU}{dE}\right|_0 (E - E_0) = U_0 + \left.\frac{dU}{dE}\right|_0 E_0 \delta \tag{5.36}$$

giving

$$\dot{\delta} = -\frac{2\pi f_{\text{rf}} e V_0 \sin(\phi_s)}{T_0 E} \tau + \frac{1}{T_0} \left.\frac{dU}{dE}\right|_0 \delta. \tag{5.37}$$

Leaving the term dU/dE unevaluated for now, the equation of motion for δ is

$$\ddot{\delta} + \frac{1}{T_0} \left.\frac{dU}{dE}\right|_0 \dot{\delta} + \frac{2\pi \alpha_c f_{\text{rf}} e V_0 \sin(\phi_s)}{T_0 E} \delta = 0. \tag{5.38}$$

The general solution for δ is then

$$\delta = A \exp\{-\alpha_s t\} e^{i(\Omega_s t + \phi_0)}, \tag{5.39}$$

where the damping rate is

$$\alpha_s = \frac{1}{2T_0}\left.\frac{dU}{dE}\right|_0. \tag{5.40}$$

The calculation of dU/dE or dP_γ/dE is complicated by the fact that particles with different energy than E_0 will travel on a dispersion orbit where the fields may be different. This occurs when a gradient is designed into the field of a dipole magnet, which is an option for damping rings that is used in the New Linear Collider (NLC). Also if the dipoles are sector magnets, then the path length increases with energy, producing another correction term. Omitting these terms for simplicity we get

$$\frac{dP_\gamma}{dE} \approx \frac{\partial P_\gamma}{\partial E} = 2\frac{P_\gamma}{E} \tag{5.41}$$

from $P_\gamma \sim E^2B^2$.

Therefore the damping rate is

$$\alpha_s = \frac{1}{T_0}\frac{U}{E}. \tag{5.42}$$

Writing in terms of P_γ, we have

$$\alpha_s = \frac{\langle P_\gamma \rangle}{E}. \tag{5.43}$$

The damping time is

$$\tau_s = \frac{1}{\alpha_s} = \frac{E}{\langle P_\gamma \rangle}, \tag{5.44}$$

the time required to radiate all the energy of the particle if there were no rf cavities to maintain the energy and $\langle P_\gamma \rangle$ stayed constant.

Gradients in dipole magnets and sector magnets require the correct expression,

$$\alpha_s = \frac{1}{2T_0}\frac{U}{E}(2+\vartheta), \tag{5.45}$$

where

$$\vartheta = \left[\int \frac{1}{\rho}(2k + \frac{1}{\rho^2})\eta\, ds\right] \Big/ \left[\int \frac{1}{\rho^2}\right]. \tag{5.46}$$

In some accelerators that have gradients in bends, ϑ is order unity, which is a significant effect.

5.3.4 Damping of Transverse Oscillations

The damping of transverse oscillation is a little simpler to illustrate. The process appears to be different, but it turns out that the result is the same as in the longitudinal case except for a factor of 2.

Starting with general transverse coordinates (x, $x' = p_x/p_z$, y, $y' = p_y/p_z$), a particle emits photons at various phases of the betatron oscillation. We assume that the photons are emitted in the direction of motion so that the angles $x' = p_x/p_z$ and $y' = p_y/p_z$ are preserved after every emission. This is a good approximation since the opening angle of photon emission is of the order $1/\gamma$, which is much less than the angular divergence of the beam. Figure 5.8 shows the damping process with nonzero transverse momentum in the vertical plane.

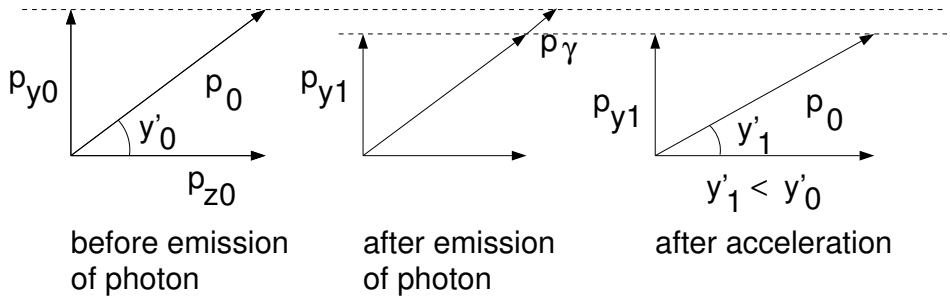

Figure 5.8: Snapshots of particle momentum showing transverse damping.

The rf cavity fields will restore the original total momentum after one turn. The fields are longitudinal and can only add to p_z. Thus we have a damping mechanism, since at every turn p_x and p_y decrease while p_z increases.

Looking at only the vertical plane, after radiating the average amount of photons over one turn and before reaching the rf cavities, the change in p_y and p_z are

$$\Delta p_y = -p_y(U_0/E_0) \text{ and} \tag{5.47}$$

$$\Delta p_z = -p_z(U_0/E_0), \tag{5.48}$$

while y' is unchanged from the radiation process. (The equations say that the momentum fractions are equal to the energy fraction lost to photon emission.) Going through the rf cavity, p_z is incremented by U_0/c, changing the angle

$y' = p_y/p_z$ by

$$\Delta y' = p_y \left(\frac{1}{p_z + U_0/c} - \frac{1}{p_z} \right) \tag{5.49}$$

$$\approx -\frac{p_y}{p_z} \frac{U_0}{cp_z} \approx -y' \frac{U_0}{E_0}. \tag{5.50}$$

The amplitude of the vertical motion is decreased at the rf cavity only when the particle has a slope there. The reduction in the invariant $A_y = \beta_y y'^2 + 2\alpha_y y y' + \gamma_y y^2$ (assume α_y=0 for simplicity) is

$$\Delta A_y = 2\beta_y y' \Delta y' \tag{5.51}$$

$$= -2\beta_y y'^2 \frac{U_0}{E_0}. \tag{5.52}$$

Averaging over phases of y' (i.e., several turns),

$$\langle \Delta A_y \rangle = -2\beta_y \langle y'^2 \rangle \frac{U_0}{E_0}. \tag{5.53}$$

But $\langle y'^2 \rangle = A_y \gamma_y / 2$ and $\gamma_y = 1/\beta_y$, then

$$\langle \Delta A_y \rangle = -A_y \frac{U_0}{E_0}. \tag{5.54}$$

Converting to a time derivative,

$$\dot{A}_y = -A_y \frac{U_0}{T_0 E_0}. \tag{5.55}$$

The time decrement for the coordinates y or y' is then

$$\alpha_y = \frac{1}{2} \frac{U_0}{T_0 E_0}. \tag{5.56}$$

This is the same time decrement in the longitudinal plane, apart from a factor of 2.

A similar derivation can be done for the horizontal plane. However the presence of a gradient in the dipole complicates things, which results in a numerical correction term for the damping decrement,

$$\alpha_x = \frac{1}{2} \frac{U_0}{T_0 E_0} (1 - \vartheta), \tag{5.57}$$

where ϑ is the same quantity in the energy damping decrement. Note that one could design a nonzero gradient and wedges on the dipole magnet to increase the damping in the horizontal plane to improve the performance of a damping ring. However this complicates the magnet design and isn't usually used for this purpose.

There is a principle that states that the sum of damping decrements in the three directions is

$$\alpha_x + \alpha_y + \alpha_z = 2\frac{U_0}{T_0 E_0}, \tag{5.58}$$

where the lattice-dependent quantity ϑ drops out. This applies only to predetermined magnetic and accelerating rf fields that are not influenced by the motion of the particles (i.e., collective effects).

5.3.5 Quantum Excitation

Quantum excitation refers to the noise generated by the random emission of photons. The noise occurs in the horizontal and longitudinal planes. If there is vertical bending somewhere in the ring, then some noise is generated in the vertical plane, too. The quantum excitation is the main process that keeps the beam emittances in the horizontal and longitudinal planes from shrinking to zero.

As a starting point, suppose that all electrons have the same energy and are traveling along the ideal orbit. After emitting a photon, the electron immediately starts to oscillate about a new off-momentum orbit corresponding to the lower energy of the electron. The coordinates of the particles don't change but the particles are forced into betatron oscillations through

$$\Delta x = \Delta x_\beta - \eta\frac{u}{E} = 0 \tag{5.59}$$

and

$$\Delta x' = \Delta x'_\beta - \eta'\frac{u}{E} = 0, \tag{5.60}$$

where u is the photon energy. We see here how a small dispersion in the dipoles will help make the betatron oscillation small, and reduce the emittance.

Let us consider the energy oscillation first. Say that a particle already undergoes an oscillation $E(t) - E_0 = Ae^{i(\Omega_s t + \phi_0)}$, then an emission of photon of energy u, at a general phase will increase the amplitude by an average of

$$\langle \Delta A^2 \rangle = u^2. \tag{5.61}$$

The rate of change while averaging over the whole ring is

$$\left\langle \left.\frac{dA^2}{dt}\right|_Q \right\rangle = \int_0^\infty u^2 \dot{n}(u) du = \left\langle \dot{N}_{\rm ph} \langle u^2 \rangle \right\rangle_s , \tag{5.62}$$

where $\dot{n}(u)$ is the number of photons of energy u emitted in the bin du over one turn of the ring. The $\langle ... \rangle$ around u^2 refers to averaging over photon energies at a particular location in the ring, and the $\langle ... \rangle_s$ around $\dot{N}_{\rm ph}\langle u^2 \rangle$ refers to the ring average. These quantities can be calculated exactly and will be given later.

From the section on damping,

$$\left\langle \left.\frac{dA^2}{dt}\right|_D \right\rangle = -2\alpha_s \langle A^2 \rangle = -\frac{2}{\tau_s}\langle A^2 \rangle. \tag{5.63}$$

At equilibrium,

$$\left\langle \left.\frac{dA^2}{dt}\right|_D \right\rangle + \left\langle \left.\frac{dA^2}{dt}\right|_Q \right\rangle = 0. \tag{5.64}$$

Then

$$\langle A^2 \rangle = \frac{1}{2}\tau_s \left\langle \dot{N}_{\rm ph} \langle u^2 \rangle \right\rangle_s . \tag{5.65}$$

At equilibrium $\langle A^2 \rangle$ is interpreted as the probable value of A^2, the energy amplitude squared. The average of the square of the energy deviation is then $\sigma_E^2 = \langle A^2 \rangle / 2$.

A complex calculation gives

$$\dot{N}_{\rm ph} \langle u^2 \rangle = \frac{55}{24\sqrt{3}} P_\gamma u_c, \tag{5.66}$$

where u_c is the critical energy. Since $P_\gamma \sim \gamma^4$ and $u_c \sim \gamma^3$, then $\dot{N}_{\rm ph}\langle u^2 \rangle \sim \gamma^7$, a very strong dependence. The equilibrium σ_E^2 goes as γ^4, and the momentum deviation goes as γ^2.

Expressing in terms of the rms of δ,

$$\sigma_\delta^2 = \frac{\sigma_E^2}{E^2} = \frac{\tau_s}{4E^2}\left\langle \dot{N}_{\rm ph} \langle u^2 \rangle \right\rangle_s = C_q \frac{\gamma^2}{J_s} \frac{\langle |\rho^{-3}| \rangle_s}{\langle \rho^{-2} \rangle_s}, \tag{5.67}$$

where $C_q = 3.8 \times 10^{-13} m$.

The excitation in the horizontal plane is derived similarly. The emission of a photon will modify the particle's ellipse $A_\beta^2 = \beta_x x'^2_\beta + 2\alpha_x x_\beta x'_\beta + \gamma_x x_\beta^2$. Making the substitutions of the type $x_\beta \rightarrow (x_\beta + \Delta x_\beta)$ and averaging over phases (which eliminates terms linear in Δx_β and $\Delta x'_\beta$) produces

$$\Delta A_\beta^2 = \frac{u^2}{E^2}\mathcal{H}(s), \tag{5.68}$$

where

$$\mathcal{H}(s) = \beta_x \eta'^2 + 2\alpha_x \eta\eta' + \gamma_x \eta^2. \tag{5.69}$$

Again we have an expression with a u^2 that we need to average over the spectrum at each point in the ring, and then to average over the ring. This results in

$$\left\langle \left.\frac{dA_\beta^2}{dt}\right|_Q \right\rangle = \frac{1}{E^2}\left\langle \dot{N}_{\rm ph}\langle u^2\rangle \mathcal{H}(s)\right\rangle_s. \tag{5.70}$$

The damping term is

$$\left\langle \left.\frac{dA_\beta^2}{dt}\right|_D \right\rangle = -\frac{2}{\tau_x}\langle A_\beta^2\rangle \tag{5.71}$$

and

$$\langle A_\beta^2\rangle = \frac{1}{2E^2}\tau_x \left\langle \dot{N}_{\rm ph}\langle u^2\rangle \mathcal{H}(s)\right\rangle_s. \tag{5.72}$$

The quantity $\langle A_\beta^2\rangle$ is interpreted as the equilibrium ellipse amplitude. Averaging over phases, the equilibrium emittance is then $\langle A_\beta^2\rangle/2$ or

$$\varepsilon_x = \frac{\tau_x}{4E^2}\left\langle \dot{N}_{\rm ph}\langle u^2\rangle \mathcal{H}(s)\right\rangle_s \tag{5.73}$$

$$= C_q \frac{\gamma^2}{J_x}\frac{\langle |\rho^{-3}|\mathcal{H}\rangle_s}{\langle \rho^{-2}\rangle_s}. \tag{5.74}$$

Note that in the term $\mathcal{H}$ the lattice has an influence on the emittance. In most cases, the main term of interest is $\beta\eta'^2$.

5.3.6 Coupling

Since there is no bending in the vertical plane, the quantum excitation is zero, and the vertical emittance would damps almost to zero. Because of the finite $1/\gamma$ emission angle of the photons, there is some vertical oscillation excited. A more significant contribution to the vertical beam size is

small magnet misalignments, which produce some vertical dispersion. This dispersion produces quantum excitation in the vertical plane. Also the same type of misalignment induces a pure horizontal motion to transfer some of its amplitude to the vertical plane, i.e. a coupling mechanism.

This results in a nonzero equilibrium vertical emittance. We normally quantify this as a ratio times the equilibrium horizontal emittance:

$$\varepsilon_y = \frac{\kappa}{1+\kappa}\varepsilon_{x0}, \tag{5.75}$$

$$\varepsilon_x = \frac{1}{1+\kappa}\varepsilon_{x0}. \tag{5.76}$$

Linear colliders require a very small vertical beam size, therefore damping rings must be operated at small coupling. This means that care must be taken in aligning the magnets, and corrections must be made to the optics once the ring is built.

5.3.7 Formula Summary

The important formulas are rewritten here using the following traditional definitions, and revealing the γ factors:

$$I_2 = \int_{\text{dipoles}} \frac{1}{\rho^2}\, ds, \tag{5.77}$$

$$I_3 = \int_{\text{dipoles}} \frac{1}{|\rho^3|}\, ds, \tag{5.78}$$

$$I_4 = \int_{\text{dipoles}} \frac{1}{\rho}(2k + \frac{1}{\rho^2})\eta\, ds \text{ (for sector magnet)}, \tag{5.79}$$

$$I_4 = \int_{\text{dipoles}} \frac{2k}{\rho}\eta\, ds \text{ (for rectangular magnet)}, \tag{5.80}$$

$$I_5 = \int_{\text{dipoles}} \mathcal{H}\frac{1}{|\rho^3|}\, ds, \tag{5.81}$$

$$\varepsilon = C_q\gamma^2\frac{I_5}{I_2 - I_4}, \tag{5.82}$$

$$\sigma_\delta^2 = C_q\gamma^2\frac{I_3}{I_2 - I_4}, \tag{5.83}$$

where $C_q = 3.84 \times 10^{-13} m$.

The integral I_5 is related to quantum excitation, and I_2 is related to damping.

The damping times are:

$$\tau_u = \frac{4\pi}{C_\gamma} \frac{T_0}{E^3[\mathrm{GeV}^3]} \frac{1}{I_2 J_u} \text{ for } u = x,\, y,\, s, \tag{5.84}$$

where $C_\gamma = 8.85 \times 10^{-5}$ m/GeV^3, and

$$J_x = 1 - I_4/I_2, \tag{5.85}$$
$$J_y = 1, \tag{5.86}$$
$$J_s = 2 + I_4/I_2. \tag{5.87}$$

5.4 Lattice Design

The main lattice parameter is the energy of the beam since the emittance and damping have a strong dependence on energy. For the linear collider the normalized emittance ($\gamma\varepsilon$) is the figure of merit. The expressions of ε in the previous sections should be replaced by expressions for $\gamma\varepsilon$ if we want to compare the performance of rings of different energies.

The damping ring is usually composed of a repeating pattern (cells) of quadrupoles and dipoles to make the arcs. The cells are designed to give specific properties to the beam such as damping and emittance. There are two cell types that are usually considered for damping rings, the FODO cell, and the theoretical minimum emittance (TME) cell. For a given cell type, there are several parameters to decide:

- cell length, L_c;
- deflection angle per dipole magnet, θ_d, or equivalently the number of cells, N_{cell} or dipoles, N_{dip}; and
- phase advance per cell in the horizontal plane, $2\pi\mu_x$.

The quantities L_c and θ_d determine the bending radius of the dipole, $\rho \sim L_c/\theta_d$. The horizontal phase advance per cell $2\pi\mu_x$ influences the emittance. The vertical phase advance is not relevant to the emittance, but it is preferred to have it small to reduce chromatic aberrations.

The emittance of the arcs is rewritten with important factors separated:

$$\gamma\varepsilon = C_q\gamma^3 F_\varepsilon(\text{lattice}, \mu_x)\frac{\theta_d^3}{J_x}, \tag{5.88}$$

where F is a phase-advance-dependent quality factor (different for each cell type).

If we add wigglers to the ring the emittance can no longer be expressed so simply. In any case, the above expression is useful in establishing an arc cell that has good characteristics.

5.4.1 FODO Cells

The FODO cell is a simple cell with alternating polarity quadrupoles between each dipole. One can operate all the focusing quadrupoles at one gradient and the defocusing quadrupoles at another gradient, to optimize the horizontal focusing for emittance and to decrease the amount of focusing in the vertical plane for reducing sextupole strengths. The FODO cell has well-known properties, some of which can be derived analytically in the "thin-lens" approximation [3].

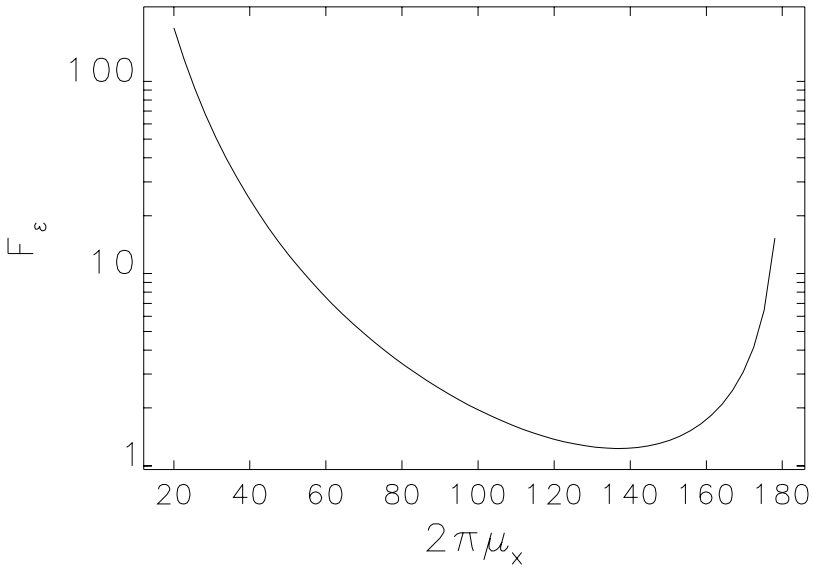

Figure 5.9: Emittance quality factor for FODO cell.

Figure 5.9 shows the quality factor for the FODO cell. The minimum value is 1.2, which is relatively high compared to other cell types. Since the curve has a broad minimum in the range 120 to 160 degrees, we could operate anywhere in that range. Actually to reduce the strength of sextupoles, it is preferable to run at the lower end of that range.

The reasons for using FODO cells are their simplicity, their flexibility (in making phase advance adjustments), generally weaker sextupoles, and the high filling factor for the dipoles needed for their damping contributions. The SLAC damping rings built in 1983 are based on optimized FODO cells and operate with phase advance per cell of 130 degrees. I presented in my 1989 thesis [4] a model damping ring that achieved an ultralow emittance with wigglers with arcs of short FODO cells, partially for simplicity of design.

5.4.2 TME Cells

In the theoretical minimum emittance cell the dispersion has a minimum in the dipole. A gradient in the dipole is optional. Quadrupoles are symmetrically placed in the cell to create a minimum for β_x. The integral of the function $\mathcal{H}$ can be minimized along the dipole. The value of the emittance quality factor is $F_\varepsilon \approx 1/12\sqrt{15} = 0.02$, about 50 times better than a FODO cell. This is understandable since these cells uses three or four quadrupoles per dipole compared to the one quadrupole per dipole in the FODO cell. When making the TME dipole angle equal to the total angle of a FODO cell with two dipoles and two quadrupoles, then the advantage is reduced by a factor of 8, obviously still substantial. At the optimum setting of the TME cell the sextupoles need to be very strong, so a "detuning" optics is often used with larger emittance to obtain weaker sextupoles.

Figure 5.10 shows the magnet layout and beta functions for the NLC damping ring. The damping ring design for TESLA uses the TME cell as well.

5.4.3 Comparison of Cells

The NLC and TESLA design groups compared the TME cell with other cells and found that the TME cell was the best choice. The TESLA group made equivalent FODO cells and TME cells by adjusting the angle per cell in each type to produce the same emittance (for example 12 degrees for TME and 7.5 degrees for FODO), and found that from simulations of particle

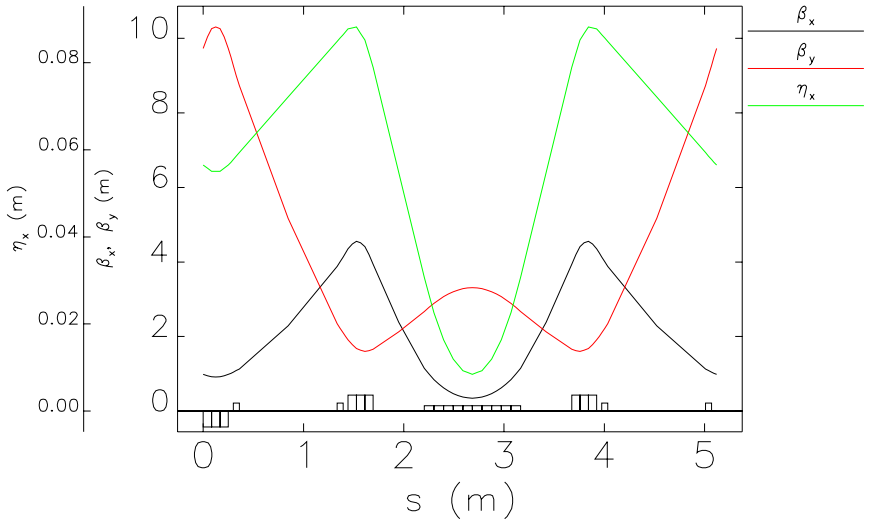

Figure 5.10: TME cell from the NLC damping ring.

trajectories the TME cell had much weaker nonlinearities from sextupole chromatic correction.

The extra space in the TME cells can be used to install hardware such as corrector dipole magnets and diagnostics.

5.5 Wiggler Design

5.5.1 Magnet Description

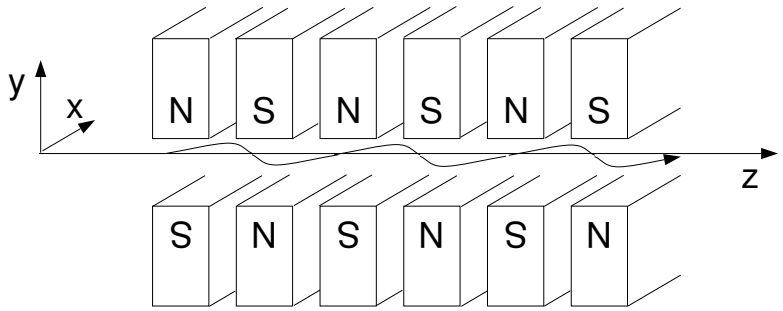

Figure 5.11: Wiggler with undulating trajectory.

A wiggler is a periodic array of poles that produces an alternating vertical field along the direction of the beam (see Figure 5.11). The wigglers are inserted in specially-reserved, dispersion-free straight sections in order to increase the damping rate by a large factor, and to decrease the emittance by about the same factor. The damping is achieved by emission of radiation as in any other bending magnet, except here the average magnetic fields are particularly high and the wigglers extend for many meters without generating a large dispersion value.

The bending radius of the wiggler is given by its magnetic field. Design teams usually select a permanent magnet wiggler design over an electromagnet design since the latter would consume too much electrical power. For the Samarium-Cobalt hybrid wiggler [5], the magnetic field is

$$B_{\max}[T] = B_0 \exp\left[-\frac{g}{l_{\rm p}}\left(2.74 - 0.45\frac{g}{l_{\rm p}}\right)\right], \tag{5.89}$$

with $B_0 = 3.33$ T. The minimum wiggler bending radius is given by

$$\frac{1}{\rho_{\rm w}} = eB_{\max}/cp. \tag{5.90}$$

The peak field depends on the wiggler gap g and period length $2l_{\rm p}$. The requirement of getting the highest peak field (for damping) implies a small gap or a long period length. Both of these are bad; the first one is not consistent with a large aperture, and the second one increases dispersion in the wiggler, which increases quantum excitation of betatron oscillations. Therefore we must choose a compromise in these variables by optimizing the emittance.

Because the wiggler generates only a small internal dispersion function, the quantum excitation is naturally small to begin with. The dispersion function inside the wiggler is related to the deflection angle due to one pole. For a sinusoidally varying field, the amplitude of the angle variation is

$$\theta = \frac{l_{\rm p}}{\pi\rho_{\rm w}}, \tag{5.91}$$

where $l_{\rm p}$ is the pole length and $\rho_{\rm w}$ is the minimum radius of curvature of the trajectory. The deflection of one pole is twice this, $2\frac{l_{\rm p}}{\pi\rho_{\rm w}}$. A wiggler with a small deflection angle will have a small quantum excitation.

5.5.2 Damping Contribution

The bending radius varies as a sine wave. The damping term $\langle 1/\rho^{-2}\rangle_s$ is simply $1/2\rho_{\rm w}^2$.

5.5.3 Quantum Excitation Contribution

The internal dispersion and the bending radius vary as sine waves. The integral of $\mathcal{H}/\rho^3$ is dominated by the $\beta\eta'^2$ term, the others are smaller by l_p/β and $(l_p/\beta)^2$.

The horizontal dispersion (there is no vertical dispersion) and its derivatives are

$$\eta''(s) = \frac{1}{\rho_{\rm w}} \sin\frac{\pi s}{l_{\rm p}}, \tag{5.92}$$

$$\eta'(s) = \eta'_0 - \frac{l_{\rm p}}{\pi\rho_{\rm w}}(\cos\frac{\pi s}{l_{\rm p}} - 1), \tag{5.93}$$

$$\eta(s) = \eta_0 + (\eta'_0 + \frac{l_{\rm p}}{\pi\rho_{\rm w}})s - \frac{l_{\rm p}^2}{\pi^2\rho_{\rm w}} \sin\frac{\pi s}{l_{\rm p}}, \tag{5.94}$$

where η_0 and η'_0 are the dispersion and its derivative at the entrance of the pole (s=0).

The quantum excitation integral for one pole is (using only the $\beta\eta'^2$ term)

$$\begin{aligned}\int_{1\ \rm pole} \mathcal{H}\left|\rho^{-3}\right| ds &\approx \frac{\overline{\beta} l_{\rm p}^2}{\pi^2\rho_{\rm w}^5}\int_0^{l_{\rm p}} \cos^2\frac{\pi s}{l}\left|\sin^3\frac{\pi s}{l_{\rm p}}\right| ds \\ &= \frac{\overline{\beta} l_{\rm p}^2}{\pi^2\rho_{\rm w}^5}\left(\frac{4l_{\rm p}}{15\pi}\right) = \frac{4\overline{\beta} l_{\rm p}^3}{15\pi^3\rho_{\rm w}^5}.\end{aligned} \tag{5.95}$$

Note the strong dependence on the bending radius.

5.5.4 Emittance

The contributions for the arcs (A) and the wiggler (W) can be separated in Equation (5.82):

$$\gamma\varepsilon = C_q\gamma^3\frac{I_{5\rm A} + I_{5\rm W}}{I_{2\rm A} + I_{2\rm W}}. \tag{5.96}$$

For a given arc design we can use the damping term $I_{2\rm W}$ in the denominator to greatly reduce damping times and emittance. With modest wigglers,

we can increase the damping by a factor of 2 or 3. We can control the quantum excitation $I_{5\mathrm{W}}$ term by selecting a short enough period length for the wiggler.

There is a lower limit in emittance that wigglers can provide because of their own quantum excitation. In the limit that the wiggler length is infinite, the emittance reaches a constant value which scales like

$$\begin{aligned} \gamma\varepsilon &= \gamma^3 \frac{I_{5\mathrm{W}}}{I_{2\mathrm{W}}}, & (5.97) \\ &\sim \gamma^3 \frac{l_{\mathrm{p}}^3 \beta_x / \rho_{\mathrm{w}}^5}{1/\rho_{\mathrm{w}}^2}, = \left(\frac{\gamma}{\rho_{\mathrm{w}}}\right)^3 l_{\mathrm{p}}^3 \beta_x & (5.98) \\ &\sim B_{\max}^3 l_{\mathrm{p}}^3 \beta_x, & (5.99) \end{aligned}$$

the last step coming from $1/\rho_{\mathrm{w}} = eB_{\max}/cp$. It turns out that the normalized emittance from a wiggler doesn't depend on the energy of the beam.

5.6 Design Requirements

These are brief comments on design requirements.

5.6.1 Circumference

The circumference is determined by the length of the linac bunch train. For example, the TESLA damping ring circumference is 17 km in order to fit a compressed 300-km bunch train. The NLC ring circumference is 300 m in order to fit three 100-meter trains.

5.6.2 Damping Rate

The damping rate is determined by the linac repetition frequency and the time required to damp the beam substantially close to the equilibrium emittance.

In rings with multiple bunch trains N_{T}, the damping time requirement is loosened by the factor N_{T}.

5.6.3 Normalized Emittance

This is determined from the interaction region specification. The values for various designs are of the order of 2×10^{-6} m-rad.

5.6.4 Coupling $\varepsilon_y/\varepsilon_x$

The coupling $\varepsilon_y/\varepsilon_x$ requirement is determined by the interaction region specification of beam-beam effect. The requirement is of the order of a 0.5% ratio. If the ring had no magnet errors, then the vertical emittance would be practically zero. However with magnet rotations, some of the horizontal motion is transfered to the vertical plane, thus giving a potentially large vertical emittance. The coupling is controlled by aligning the magnets well and by applying optics corrections with skew quadrupole magnets.

5.6.5 Operating Energy

The energy is usually determined by the emittance and damping requirements, which was done in the SLAC Linear Collider (SLC) damping rings. Sometimes the energy is adjusted to reduce instabilities in general. The energy may be reduced to save costs if it is a relatively free parameter.

5.7 Limitations

There are limitations in the implementation of the requirements mentioned in the previous section that will require an adjustment to an initial design.

5.7.1 Dynamic Aperture

A cell with low dispersion and strong focusing will need strong sextupoles. The TME cell is such a case. The TME cell is usually "detuned" to make the dispersion at the sextupoles larger, thus decreasing their strength.

5.7.2 Emittance Blow-Up from IBS

Intrabeam scattering (IBS) is the internal scattering of particles from collisions in each bunch. In the beam frame, the distributions of momenta along the three axes are quite different. The effect is to increase the emittance and

energy spread as the bunch charge increases. The original distribution of the momenta along the three axes for the model damping ring of my thesis are:

$$\sigma_{p_x} \sim \sqrt{\varepsilon\beta_x}p_0 \approx 1.6 \times 10^{-6}p_0, \quad (5.100)$$

$$\sigma_{p_s} \sim \sigma_\delta p_0/\gamma \approx 1 \times 10^{-7}p_0. \quad (5.101)$$

Particles will preferentially scatter pairwise into opposite s directions (on the average), thus increasing the energy spread σ_{p_s}, and, at first sight, reducing the horizontal momentum spread σ_{p_x}. However a large fraction of the scattering occurs where there is dispersion. The sudden change in momenta for both colliding particles excites a horizontal betatron motion in both, thus increasing the horizontal momentum spread (and horizontal emittance. The intrabeam scattering growth rate goes as $1/\gamma^4$, therefore the growth is much reduced at higher operating energies.

This is an ongoing process that is limited in electron storage rings by radiation damping. The equilibrium horizontal emittance increase goes as $1/\gamma^4$.

5.8 Implementations

The implementations of damping ring design requirements in various damping rings are described below. Table 5.1 lists the main design parameters for these damping rings. For understanding the effects of the wiggler, the second and third rows list the normalized emittance contributions from the ring arcs and wigglers. The second row denoted "$\gamma\varepsilon$ of arcs only" refers to the emittance of the ring with the wigglers turned off. The third row "$\gamma\varepsilon$ of wigglers" refers to the limiting emittance if the wigglers were of infinite length, or if the arcs didn't produce any quantum excitation. The real emittance in the first row is a value in between. In the seventh row, ε refers to the geometrical equilibrium emittance.

The implementations are the result of compromise between requirements. Reference [6] reports on the systematic approach that balances the design requirements with the feasibility of the design. The reader is invited to read this paper as a continuation of this lecture.

Table 5.1: Some Parameters of the Damping Rings Mentioned

	SLC	NLC	TESLA	Emery's thesis
$\gamma\varepsilon$ (m-rad)	2.1×10^{-5}	3×10^{-6}	8×10^{-6}	2.0×10^{-7}
$\gamma\varepsilon$ (m-rad) of arcs only	2.1×10^{-5}		3.7×10^{-5}	2.7×10^{-6}
$\gamma\varepsilon$ (m-rad) of wigglers	n/a		2.4×10^{-6}	1.1×10^{-7}
L_{W} (m)	0	46	468	360
$F_{\mathrm{W}} = I_{2\mathrm{W}}/I_{2\mathrm{A}}$	0	2.15	17.3	32
Injected $\gamma\varepsilon$ (m-rad)	5×10^{-3}	1.5×10^{-4}	10×10^{-6}	n/a
ε (m-rad)	9×10^{-9}	8×10^{-10}	8×10^{-10}	2.5×10^{-11}
Energy (GeV)	1.2	1.98	5.0	4.0
Circumference (m)	35	300	17000	2229
τ_x (ms)	3.0	4.9	28	13.5
$\tau_{x,\mathrm{T}} = \tau_x/N_{\mathrm{T}}$ (ms)	3.0	1.7	28	0.61[†]

[†] Used the same length of train as the NLC damping ring.

5.8.1 SLC

The SLAC linear collider was designed with two small damping rings [7] operating at 1.2 GeV. They are made with short FODO cells with 2-T dipole magnets. There are no wigglers in the design.

5.8.2 NLC

The NLC operates at 120 Hz, which requires a damping rate much less than the pulse interval of 8 ms. The circumference of the damping ring (300 m) allows storing of three bunch trains, effectively extending the time for damping by a factor of 3. The bunch train of the NLC is 190 bunches at 1.4-ns intervals. The NLC damping ring operates at 1.98 GeV. Some 46 meters of wiggler are included to produce a sufficiently small damping time of about 5 ms.

There is an additional predamping ring, to damp the rather large-emittance positron beam before the positron beam can be accepted without loss by the main damping ring.

The normalized emittances are $\gamma\epsilon_x = 3$ mm-rad and $\gamma\epsilon_y = 0.02$ mm-rad. The cells in the arcs are TME cells that are adjusted to give larger dispersion

and a weaker sextupole correction.

5.8.3 TESLA

The TESLA linear collider accelerates a train of 2820 bunches a total of 1 ms long. The bunch train length would be 300 km, which would have required a damping ring with a circumference of the same length. However, by storing the bunch train in a compressed mode, one can reduce the circumference of the ring. The limitation is the quickness of the injection and ejection pulsed magnets. With a 20-ns rise time, it is possible to fit 300 km of bunch train into 17 km. In order to save tunneling costs, the long straight sections of the damping ring are squeezed together to fit inside the linac tunnel, leaving two arcs sections in their own circular tunnels, forming a "dog-bone" layout.

The cycle time for the linac is 0.2 s, therefore the damping time requirement isn't as strong as the NLC. The damping time is set at 25 ms (50 ms for electrons, i.e., half the wigglers, since electrons don't have to damp as much).

The energy is 5 GeV, significantly higher than the SLC. This value was selected to reduce the space-charge tune shift, which goes as $C/(\gamma^2\sigma_x\sigma_u)$ for $u = x,\ y$, where C is the circumference. The effect is particularly strong because of the large circumference and the low emittance. The higher energy also greatly reduces the effect of intrabeam scattering, which is a mechanism for emittance growth.

The rest of the parameters, ρ, θ_{cell}, and the ratio F_{cell} are set by the damping time and the emittance and by minimizing the wiggler length.

5.8.4 Ultralow Emittance Model Ring

This damping ring was designed for my thesis as an exercise to see how far we can go in lowering the emittance with a large circumference ring, many FODO cells, realistic magnets, and lots of wigglers. There were no emittance or damping requirements except that they were to be much stronger than the requirements discussed at the time (1988).

I set the FODO cell length to 7.2 m, the phase advance per cell to 90 degrees, and the length of the wiggler at 360 m. I minimized the emittance using the period length of the wiggler for a fixed gap. The contributions of arc and wigglers to the damping and quantum excitation are shown in Table 5.2.

Table 5.2: Damping and Quantum Excitation Contributions from Arcs and Wigglers in Thesis Damping Ring.

	Arc	Wigglers
I_2 (m^{-1})	5.6×10^{-7}	7.4×10^{-7}
I_5 (m^{-2})	3.8×10^{-2}	1.2

The contributions to quantum excitation from arcs and wiggler end up being about the same, while the damping is provided by the wigglers only.

5.9 Acknowledgements

Much of the derivations that appear in these notes comes from references [8] and [9].

Bibliography

[1] W. Decking. Optical Layout of the TESLA 5GeV Damping Ring. Tesla report 2001-11, web page http://tesla.desy.de/new_pages/tesla_reports/2001/pdf_files/tesla2001-11-1.pdf., February 2001.

[2] Andrzej Wolski. Lattice Description for NLC Main Damping Rings at 120 Hz. CBP Tech Note 227, LBL.

[3] H. Wiedemann. Scaling of FODO-Cell Parameters. PEP-note 39, SLAC, August 1973.

[4] Louis Emery. *A Wiggler-Based Ultra-Low Emittance Damping Ring and Its Chromatic Correction*. PhD thesis, Stanford University, 1990.

[5] K. Halbach. Permanent Magnet Undulators. In *Proceedings of the Bendor Free Electron Laser Conference. Journal de Physique. Suppl. #2*, volume 44, pages C1–211, 1983.

[6] Paul Emma and Tor Raubenheimer. Systematic Approach to Damping Ring Design. *Physical Review Special Topics - Accelerator and Beams*, 4, 2002.

[7] G.E. Fischer, W. Davies-White, T. Fieguth, and H.Wiedemann. A 1.2 GeV Damping Ring Complex for the Stanford Linear Collider. In *Proceedings of the 12th International Conference of High-Energy Accelerators*, August 1983.

[8] Matthew Sands. The physics of Electron Storage Rings, An Introduction. SLAC 121, SLAC, November 1970.

[9] H. Wiedemann. *Particle Accelerator Physics*. Springer-Verlag, 1993.